Inflammation, Vol. 41, No. 1, February 2018 (© 2017)
DOI: 10.1007/s10753-017-0659-5

ORIGINAL ARTICLE

A Novel Role of a Chemotherapeutic Agent in a Rat Model of Endotoxemia: Modulation of the STAT-3 Signaling Pathway

Omnia S. Zaki,[1,5] Marwa M. Safar,[2,3] Afaf A. Ain-Shoka,[2] and Laila A. Rashed[4]

Abstract— Sepsis caused by lipopolysaccharide (LPS) is a life-threatening disease accompanied by multiple organ failure. This study investigated the curative effects of imatinib (IMA) against hepatic, renal, and pulmonary responses caused by a single administration of LPS (10 mg/kg, i.p.) in rats. Treatment with IMA (15 mg/kg, i.p.) 30 min after LPS antagonized the LPS-induced boost of liver enzymes (ALT, AST), kidney functions (BUN, sCr) as well as the elevated pulmonary vascular permeability and edema. IMA declined tissue contents of NF-κB, STAT-3, P38-MAPK, TNF-α, IL-1β, and iNOS. It also amplified the anti-inflammatory cytokine IL-10 as well as the Bcl-2/Bax ratio, a cardinal indicator of the anti-apoptotic effect. Meanwhile, the rats exhibited marked reduction of the broncho-alveolar lavage fluid (BALF) contents of TNF-α, IL-1β, IFN-γ, and neutrophil count; however, they revealed prominent augmentation of the BALF content IL-10. In conclusion, these findings suggest that IMA is endowed with anti-inflammatory, anti-oxidant, and anti-apoptotic properties and hence may provide a novel agent for the management of sepsis.

KEY WORDS: endotoxin; apoptosis; tyrosine kinase inhibitor; oxidative stress; STAT-3; toll-like receptor-4.

This work is attributed to:

1. The Department of Pharmacology and Toxicology, Faculty of Pharmacy, Modern University for technology & information (MTI), Cairo, Egypt
2. The Department of Pharmacology and Toxicology, Faculty of Pharmacy, Cairo University, Cairo, Egypt
3. The Department of Pharmacology and Biochemistry, Faculty of Pharmacy, The British University in Egypt (BUE), Cairo, Egypt
4. The Department of Biochemistry and Molecular Biology, Faculty of Medicine, Cairo University, Cairo, Egypt

[1] Department of Pharmacology and Toxicology, Faculty of Pharmacy, Modern University for technology & information (MTI), Cairo, Egypt
[2] Department of Pharmacology and Toxicology, Faculty of Pharmacy, Cairo University, Cairo, Egypt
[3] Department of Pharmacology and Biochemistry, Faculty of Pharmacy, The British University in Egypt (BUE), Cairo, Egypt
[4] Department of Biochemistry and Molecular Biology, Faculty of Medicine, Cairo University, Cairo, Egypt
[5] To whom correspondence should be addressed at Department of Pharmacology and Toxicology, Faculty of Pharmacy, Modern University for technology & information (MTI), Cairo, Egypt. E-mail: omniashafik87@gmail.com

INTRODUCTION

Sepsis is the major culprit behind systemic inflammatory response syndrome (SIRS); an overwhelming life-threatening disease [1]. SIRS is considered as one of the leading causes of death worldwide especially in the intensive care units [2]. Inevitably, it remains an important clinical problem in the future, especially in light of the surge in the aging population and the emerging antibiotic resistance. Various sepsis models are used to preliminarily test potential therapeutic treatments prior to clinical trials. Exogenous administration of a bacterial toxin, such as lipopolysaccharide, is the most widely used experimental model of toxemia [3].

Endotoxic lipopolysaccharide (LPS) is the antigenic glycolipid product found in the outer membrane of all gram-negative bacterial cell walls. It is a crucial malefactor behind septic shock in humans and has the ability to initiate a vigorous inflammatory response [4]. The effects of LPS in experimental animals and those observed in patients with gram-negative

bacterial infections are quite comparable [5]. Endotoxemia results in fever, circulatory shock, disseminated intravascular coagulation, and damage of numerous organs, including the liver [6], kidney [7], and lung [8].

LPS displays its endotoxic activity by binding with its specific exogenous ligand toll-like receptor-4 (TLR-4) that belongs to the family of pattern recognition receptors (PRRs) and plays a central role in host defenses against sepsis [9]. Cytokines are an important component of the "hyper-inflammatory" response to severe infection and play a devastating role in the progression of sepsis. Hence, elimination or inhibition of several pro-inflammatory mediators including tumor necrosis factor (TNF-α), interleukin (IL)-1β, IL-12, IL-17, IL-18, interferon-γ (IFN-γ), and macrophage migration inhibitory factor improves survival in sepsis models [10]. Interestingly, this endotoxin triggers excessive production of the signal transducers and activators of transcription (STAT) protein family, specifically STAT-3, which is involved in the upregulation of lipopolysaccharide binding protein, leading to amplification of inflammation in sepsis [11].

Imatinib (IMA) is an antineoplastic agent which inhibits different tyrosine kinases depending on the type of cancer. It has been approved by the U.S. Food and Drug Administration as the first-line therapy for treating chronic myeloid leukemia (CML) by blocking break point cluster region-abelson kinase (bcr-abl) activity rather than non-specifically inhibiting and killing all rapidly dividing cells [12]. IMA selectively and competitively blocks the adenosine triphosphate (ATP) binding sites of several tyrosine kinases, including stem cell factor receptor (c-Kit), abelson kinase (c-Abl), or platelet-derived growth factor (PDGF), preventing substrate phosphorylation which in turn inhibits cellular proliferation [13].

IMA has been reported to possess beneficial pharmacological effects as anti-inflammatory and anti-fibrotic effects in humans [14] and in experimental animals [15]. Moreover, this drug hinders LPS-mediated phosphorylation of the regulatory protein inhibitory kappa B (IκB), with subsequent prevention of the transcription factor nuclear factor kappa B (NF-κB) activation [16]. IMA is considered as an inimitable pharmacologic agent in the treatment of gram-negative sepsis and sepsis-induced acute respiratory distress syndrome (ARDS) [17]. It was reported that IMA rapidly resolves pulmonary edema *via* attenuation of pulmonary endothelial barrier dysfunction caused by histamine, thrombin, and intratracheal LPS [18, 19]. Furthermore, as protein kinases play a pivotal role in renal inflammation and fibrosis, IMA has been demonstrated to be a renoprotective drug in rats and ameliorates renal fibrosis by inhibition of c-abl activity [20].

In an attempt to identify new drugs to counteract SIRS, the current study was conducted to investigate the efficacy of IMA in a LPS-induced sepsis model in rats, addressing the modulation of TLR-4-induced inflammation, oxidative stress, and apoptotic signaling cascade.

MATERIALS AND METHODS

Animals

Adult male Wistar albino rats, weighing 120–180 g, were used in the present study; they were purchased from El Nile Pharmaceutical Company (Cairo, Egypt). The rats were housed in plastic cages for at least 1 week for acclimatization in the animal house at the Faculty of Pharmacy, Cairo University. The animals were kept under controlled environmental conditions during the experimentation period; constant temperature (25 ± 2 °C), humidity (60 ± 10%), and alternating 12 h light-dark cycles. The standard pellet diet and water were allowed *ad libitum*. The investigation was approved by the Ethics Committee for Animal Experimentation of Pharmacy, Cairo University (Permit number: PT 599) and complies with the Guide for Care and Use of Laboratory Animals published by the US National Institutes of Health (NIH Publication No. 85-23, revised 1996).

Experimental Design

The rats were divided into three groups with eight rats each. Group 1 received normal saline and served as the control group. The rest of the animals received LPS (extracted from *Escherichia coli* 0111:B4; Sigma, St. Louis, MO) intraperitoneally in a dose of 10 mg/kg [21]. The rats of the second group were left untreated while, group 3 was given IMA (Novartis, Basel, Switzerland) intraperitoneally [22] 30 min after LPS exposure as a single dose of 15 mg/kg which was converted from mice (30 mg/kg) [23] to rats according to the assumptions and constants of the paper by [24]. In addition, when imatinib was injected alone, it showed no changes, the same as compared to the control group.

Broncho-alveolar lavage fluids (BALFs) were collected from the right lung of each rat just before the animal's decapitation. Blood samples were withdrawn from the retro-orbital plexus of each rat 24 h after LPS, collected in heparinized capillary tubes [25] on ice, and then centrifuged immediately at 3000 rpm for 20 min at 4 °C (Hettich Universal 32R, Germany). Serum was used for the estimation of alanine aminotransferase (ALT), aspartate aminotransferase (AST), serum creatinine (sCr), and blood urea nitrogen (BUN). Each sample was divided into several aliquots, one for each estimated parameter to

avoid freezing and thawing. Serum aliquots were stored at −20 °C until they were assayed later.

Immediately after collection of the blood samples, the animals were sacrificed by decapitation; livers, kidneys, and lungs were removed and washed with saline. A part of each liver, the left kidney, and the left lung which was used to determine lung water content were weighed and homogenized using a homogenizer (ART-MICCRA D-8, Germany) with ice-cold phosphate buffer saline (PBS) to prepare (1:10 *w*/*v*) homogenate. Homogenates were centrifuged at 4000 rpm at 4 °C for 15 min, and the supernatants were frozen at −80 °C until they were assayed later for estimation of upstream inflammatory cytokines namely NF-κB, STAT-3, and P38-mitogen-activated protein kinase (P38-MAPK); downstream inflammatory cytokines namely TNF-α, interleukin-1β (IL-1β), and inducible nitric oxide synthase (iNOS); anti-inflammatory cytokine namely interleukin-10 (IL-10); and apoptotic proteins namely Bax and B-cell lymphoma 2 (Bcl2).

Isolation of Broncho-Alveolar Lavage Fluid (BALF)

The animals were anesthetized 24 h after LPS injection with an intraperitoneal injection of sodium pentobarbital (50 mg/kg). A thoracotomy was performed to expose the lungs and the trachea; a cannula was inserted into the trachea and secured using a silk suture, then 12 mL of phosphate-buffered saline (0.9% NaCl-50 mM phosphate, pH 7.4) was injected into the right lung *via* a syringe and the tracheal cannula. The infusion was allowed to remain for 30 s, retrieved, and then reinstilled for a total of three washes with the same solution. An average of 9 mL BALF was recovered from each rat [26]. BALF was centrifuged at 800*g*, and the supernatant was stored at −70 °C immediately for detection of inflammatory cytokines namely TNF-α, IL-1β, IL-10, and IFN-γ. The deposited cells were resuspended in 0.2 mL PBS, and the neutrophil cell counts were determined on BALF smear slides that were stained with Hemacolor (EMD Chemicals, USA).

Lung Water Content Estimation

The lungs were dissected immediately after anesthesia by an intraperitoneal injection of sodium pentobarbital (50 mg/kg). The left lung from each animal was washed with normal saline to remove residual blood and weighed to obtain the wet lung weight and then dried in a drying oven at 80 °C for 12 h and weighed again to obtain the dry lung weight. The values obtained were used to determine the wet/dry weight ratios [27].

Biochemical Measurements in Serum

Liver and Kidney Functions

ALT, AST, sCr, and BUN levels were determined according to the manufacturer's prescripts using reagent kits (Biodiagnostic Company, Egypt).

Biochemical Measurements in Liver, Lung, and Kidney Homogenates and BALFs

Cytokine Determination

IL-1β and TNF-α levels in the liver, lung, and kidney homogenates and BALFs were determined using commercial ELISA rat kits supplied by R&D Systems (USA) according to the methods by [28] and [29], respectively. IL-10 contents in the liver, lung, and kidney homogenates and BALFs as well as IFN-γ levels in BALFs were determined using commercial ELISA rat kits supplied by MyBiosource (USA) according to the methods by [30] and [31], respectively.

Western Blot Analysis of Liver, Lung, and Kidney NF-κB, P38-MAPK, and STAT-3 Protein Expressions

Proteins from the liver, lung, and kidney tissues were extracted with lysis buffer (radioimmunoprecipitation assay (RIPA) buffer with protease and phosphatase inhibitor) on ice for 30 min on a shaker. Cell debris was removed by centrifugation at 16,000×*g* for 30 min at 4 °C. The supernatant was transferred to a new tube for further protein concentration determination analysis. The Bradford Protein Assay Kit (SK3041) for quantitative protein analysis was provided by BIO BASIC INC. (Markham, Ontario, Canada). A 20-μg protein concentration of each sample was loaded with an equal volume of Laemmli sample buffer. An aliquot of 7.5 μg protein of each sample was boiled with Laemmli buffer at 95 °C for 5 min to ensure that proteins were denatured, then each sample was loaded into an individual lane in sodium dodecyl sulfate polyacrylamide gel electrophoresis (SDS-PAGE) and transferred to polyvinylidene (PVDF) membranes. The membranes were blocked with blocking solution that was composed of tris-buffered saline with Tween 20 (TBST) buffer and 3% bovine serum albumin (BSA) for 1 h at room temperature and incubated with primary antibody diluted in TBST against the blotted target protein overnight at 4 °C. The blot was rinsed three to five times for 5 min with TBST.

After that, the incubation was done in the peroxidase-conjugated secondary antibody (goat antirabbit IgG-HRP-1 mg goat mab—Novus Biologicals) solution against the blotted target protein for 1 h at room temperature. The blot was rinsed three to five times for 5 min with TBST. Protein bands were visualized using an enhanced chemiluminescence (ECL) system (Clarity™ Western ECL substrate—BIO-RAD, USA). The chemiluminescent signals were captured using a CCD camera-based imager. Image analysis software was used to read the band intensity of the target proteins against the control sample by normalization to β-actin on the ChemiDoc MP imager (BIO-RAD, USA).

Quantitative Real-Time Polymerase Chain Reaction (qPCR) for Liver, Lung, and Kidney iNOS, Bax, and Bcl2 Contents

Total RNA was extracted from the liver, kidney, and lung tissues using the SV Total RNA Isolation System (Promega, Madison, WI, USA), and the purity of the obtained RNA was verified spectrophotometrically at 260 nm. The extracted RNA was reverse transcribed into complementary DNA (cDNA) using a reverse transcriptase-polymerase chain reaction (RT-PCR) kit (Stratagene, USA) according to the manufacturer's instructions. To assess the expression of iNOS, Bax, and Bcl2 target genes, quantitative real-time PCR was performed using SYBR Green PCR Master Mix (Qiagen, Germany) as described by the manufacturer. Briefly, 25 μL of QuantiFast SYBR Green Master Mix, 22.5 μL dH_2O, 2 μL primer pair mix (5 pmol/μL each primer), and 0.5 μL cDNA in a final reaction volume of 50 μL were used. The sequences of primers of iNOS, Bax, and Bcl2 genes and housekeeping gene β-actin are listed in Table 1.

PCRs included 10 min at 95 °C for activation of AmpliTaq DNA polymerase, followed by 40 cycles at 95 °C for 15 s (denaturing) and 72 °C for 10 min (annealing/extension). Data were expressed in cycle threshold (C_t) where the increased fluorescence curve passes across a threshold value. The relative expressions of target genes were obtained using the comparative C_t ($\Delta\Delta C_t$) method. The ΔC_t was calculated by subtracting β-actin C_t from that of the target gene whereas $\Delta\Delta C_t$ was obtained by subtracting the ΔC_t of the reference sample (internal control) from that of the test sample. The relative expression ratios were calculated by $2^{-\Delta\Delta C_t}$ [32].

Histopathological Examination

After fixation in 10% formol saline for 24 h, the liver and kidney tissues were washed under tap water, then serial dilutions of alcohol (methyl, ethyl, and absolute ethyl) were used for dehydration. The specimens were cleared in xylene and embedded in paraffin at 56 °C in a hot-air oven for 24 h. Paraffin beeswax tissue blocks were prepared for sectioning at 4 μm thickness by a slide microtome. The obtained tissue sections were collected on glass slides, deparaffinized, and stained by hematoxylin and eosin (H&E) stain for examination through a light electric microscope [33].

Statistical Analysis

Data were expressed as means ± standard error of the mean (SEM) except BALF neutrophil count data that were expressed as medians ± (range). Comparisons between means were carried out using one-way analysis of variance (ANOVA) followed by Tukey's multiple comparison test, while comparisons between medians were carried out using Kruskal-Wallis non-parametric one-way ANOVA followed by Dunn's multiple comparison test. Statistical analysis was performed using GraphPad Prism software (version 5); a probability level of less than 0.05 was accepted as statistically significant.

Table 1. Sequence of the Primers Used for Real-Time PCR

Parameter	Primer sequence	Gene bank accession number
iNOS	Forward: 5′ GACTGTTGCTCCCCCTTACC 3′ Reverse: 5′ ACAAGTCACATCGCCTTCGT 3′	XM_006287537.1
Bcl2	Forward: 5′ ATCGCTCTGTGGATGACTGAGTAC 3′ Reverse: 5′ AGAGACAGCCAGGAGAAATCAAAC 3′	XM_008952707.2
Bax	Forward: 5′ TTCAACTGGGGCCGCGTGG TT 3′ Reverse: 5′ GGAGAGGAGGCCTTCCCAGCC 3′	NM_007527.3
β-actin	Forward: 5′ TGACGAGGCCCAGAGCAAGA 3′ Reverse: 5′ ATGGGCACAGTGTGGGTGAC 3′	XM_002751780.4

RESULTS

Effects of IMA on Liver Enzymes and Kidney Functions

Lipopolysaccharide-exposed rats exhibited marked impairment in both liver and kidney functions, with serum ALT-, AST-, creatinine-, and BUN-level elevation by 3.6-fold, 3-fold, 3.6-fold, and 2.5-fold of normal values, respectively. Treatment with IMA antagonized the increase in ALT levels by 34.9% and reverted AST, sCr, and BUN levels back to their normal levels (Fig. 1a, b).

Effects of IMA on Some Liver, Kidney, and Lung Upstream Inflammatory Biomarker Contents

LPS administration caused eminent elevations of hepatic NF-κB, STAT-3, and P38-MAPK levels by 12-fold, 9.5-fold, and 10.3-fold, respectively, as compared to the control group. Treatment with IMA totally averted the modification in NF-κB liver content while it hampered the other aforementioned inflammatory mediators by 39% (STAT-3) and 66.7% (P38-MAPK) as compared to the LPS group (Fig. 2a–c).

Protein expressions of kidney NF-κB, STAT-3, and P38-MAPK contents were obviously raised up after LPS administration as compared to control animals by 9.4-fold, 7-fold, and 8-fold, respectively. IMA normalized NF-κB, STAT-3, and P38-MAPK kidney protein expressions (Fig. 3a–c).

Endotoxemia caused a spike in lung NF-κB, STAT-3, and P38-MAPK protein expressions which amounted to 10.3-fold, 7.4-fold, and 7.8-fold, respectively, of the normal values. On the other hand, a dramatic depletion of lung NF-κB (68.7%), STAT-3 (50.9%), and P38-MAPK (51.9%) protein levels was observed in IMA-treated rats as compared to the LPS group (Fig. 4a–c).

Effects of IMA on Some Liver, Kidney, and Lung Downstream Inflammatory Biomarker Contents

Table 2 depicts the effects of IMA on some liver downstream inflammatory biomarker contents. LPS-subjected animals demonstrated a pronounced elevation in TNF-α and IL-1β liver contents which reached 4.4-fold and 3-fold, respectively, of the values of the normal ones. On the contrary, LPS diminished IL-10 content (64.3%) as compared to normal animals. These parameters were normalized by IMA administration while it significantly increased the IL-10 level (92.3%) as compared to the LPS group.

Table 3 depicts that endotoxemic rats subjected to LPS exhibited prominent elevations in the kidney TNF-α (2.5-fold) and IL-1β (3.3-fold) contents as compared to the control partners. On the other hand, a significant decrease in kidney IL-10 content was revealed after LPS injection by 46.9% as compared to the control animals. Notably, IMA administration normalized both TNF-α and IL-1β as compared to the control group. The IMA-treated group

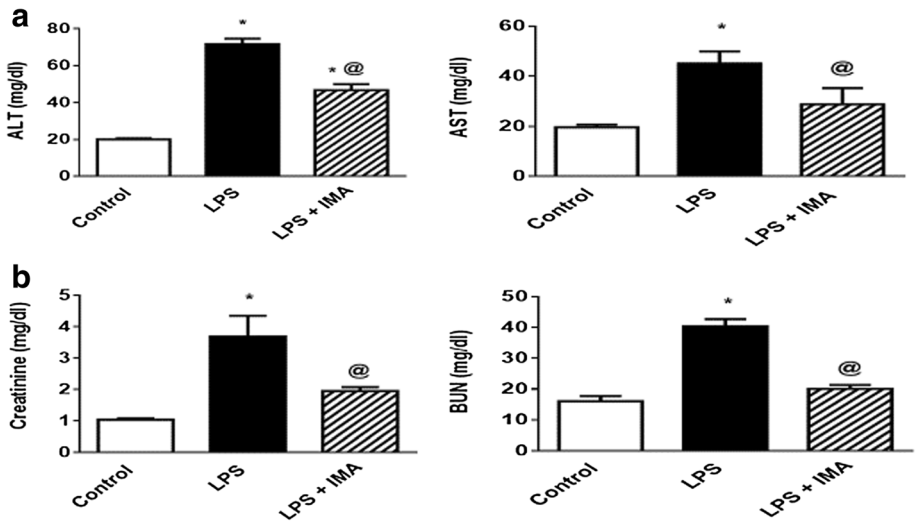

Fig. 1. Effects of IMA on liver enzymes ALT and AST (**a**) and kidney functions sCr and BUN (**b**) in rats subjected to LPS. Each bar with a vertical line represents the mean ± SEM of six to eight rats per group. Asterisk, *vs.* the control group and at sign, *vs.* the LPS group (one-way ANOVA followed by Tukey's multiple-comparison test; $P < 0.05$). LPS, lipopolysaccharide; IMA, imatinib.

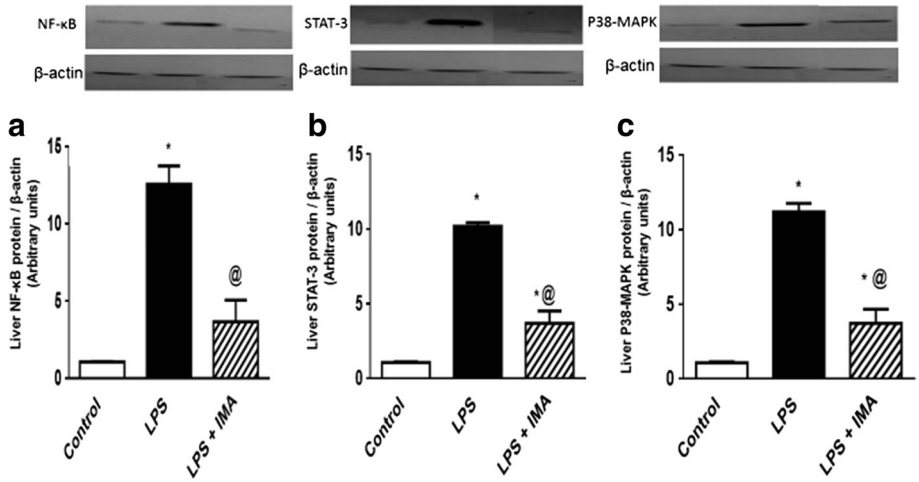

Fig. 2. Effect of IMA on liver contents of NF-κB (**a**), STAT-3 (**b**), and P38-MAPK (**c**) in rats subjected to LPS. The protein levels were quantified by western blot analysis and normalized with their respective β-actin level. Each bar with a vertical line represents the mean ± SEM of six to eight rats per group. Asterisk, *vs.* the control group and at sign, *vs.* the LPS group (one-way ANOVA followed by Tukey's multiple-comparison test; $P < 0.05$). LPS, lipopolysaccharide; IMA, imatinib; NF-κB, nuclear factor-κB; STAT-3, signal transducers and activators of transcription-3; P38-MAPK, P38-mitogen-activated protein kinase.

showed an increment in IL-10 content, but it did not markedly affect the IL-10 level as compared to LPS.

Table 4 depicts the effects of IMA on some lung downstream inflammatory biomarker contents. The TNF-α and IL-1β lung contents were significantly augmented by 3.9-fold and 3.7-fold, respectively, after LPS exposure as compared to the control animals, while LPS hampered lung IL-10 content markedly by 51.2% as compared to the normal counterparts. IMA caused prominent reductions in the lung TNF-α (32.2%) and IL-1β (39.6%) contents as compared to the LPS group. Inversely, IMA caused a significant increment in the lung IL-10 content by 61% as compared to the LPS group.

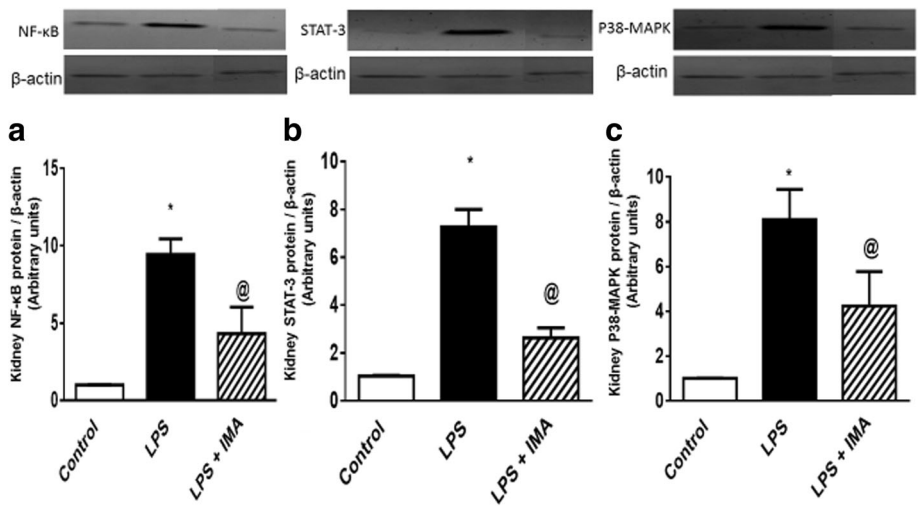

Fig. 3. Effect of IMA on kidney contents of NF-κB (**a**), STAT-3 (**b**), and P38-MAPK (**c**) in rats subjected to LPS. The protein levels were quantified by western blot analysis and normalized with their respective β-actin level. Each bar with a vertical line represents the mean ± SEM of six to eight rats per group. Asterisk, *vs.* the control group and at sign, *vs.* the LPS group (one-way ANOVA followed by Tukey's multiple-comparison test; $P < 0.05$). LPS, lipopolysaccharide; IMA, imatinib; NF-κB, nuclear factor-κB; STAT-3, signal transducers and activators of transcription-3; P38-MAPK, P38-mitogen-activated protein kinase.

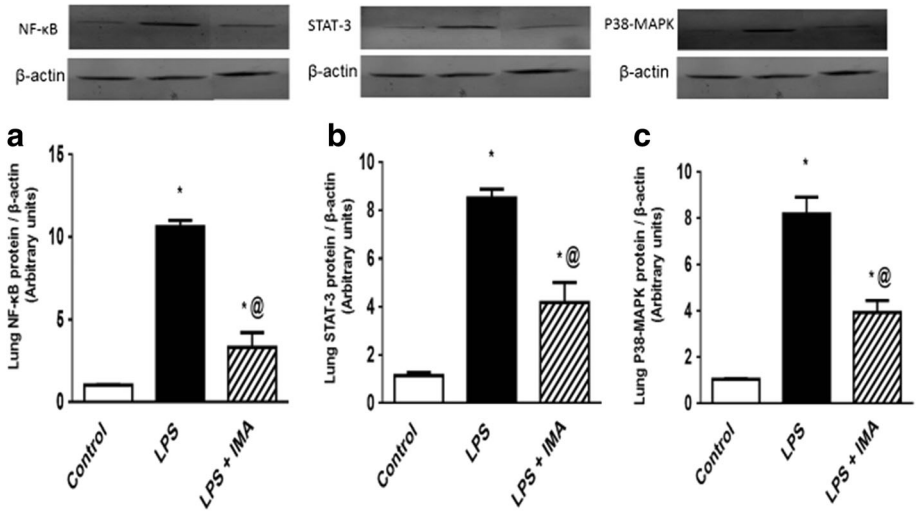

Fig. 4. Effect of IMA on lung contents of NF-κB (**a**), STAT-3 (**b**), and P38-MAPK (**c**) in rats subjected to LPS. The protein levels were quantified by western blot analysis and normalized with their respective β-actin level. Each bar with a vertical line represents the mean ± SEM of six to eight rats per group. Asterisk, *vs.* the control group and at sign, *vs.* the LPS group (one-way ANOVA followed by Tukey's multiple-comparison test; $P < 0.05$). LPS, lipopolysaccharide; IMA, imatinib; NF-κB, nuclear factor-κB; STAT-3, signal transducers and activators of transcription-3; P38-MAPK, P38-mitogen-activated protein kinase.

Effects of IMA on Liver, Kidney, and Lung iNOS Contents and Apoptotic Protein Ratios (Bcl2/Bax)

The liver, kidney, and lung contents of iNOS were significantly augmented by 13.2-fold, 9-fold, and 8.4-fold, respectively after LPS exposure as compared to control animals. Notably, IMA administration normalized the liver iNOS content as compared to the control group while it caused prominent reductions of kidney (53.9%) and lung (47.5%) iNOS contents as compared to LPS-subjected animals (Fig. 5a–c).

A pronounced depletion of liver, kidney, and lung Bcl2/Bax ratios was observed in LPS-exposed rats as compared to control ones by 98, 77.8, and 97.7%, respectively. On the contrary, IMA treatment significantly boosted the liver Bcl2/Bax ratio by 8.7-fold as compared to the LPS group. Notably, IMA did not cause significant alterations in both kidney and lung Bcl2/Bax ratios as compared to the LPS group (Fig. 6a–c).

Table 2. Effect of IMA on Liver Downstream Inflammatory Biomarker Contents in Rats Subjected to LPS

Group	Parameter		
	TNF-α (pg/g tissue)	IL-1β (pg/g tissue)	IL-10 (pg/g tissue)
Control (saline)	39.01 ± 2.04	42.99 ± 3.39	158.4 ± 10.36
LPS	172.5 ± 9.78*	135.4 ± 8.51*	56.45 ± 3.92*
LPS + IMA	69.33 ± 2.17@	66.70 ± 10.43@	108.5 ± 2.68*, @

Values are expressed as the mean ± SEM of six to eight rats per group
LPS lipopolysaccharide, *IMA* imatinib
* *vs.* the control group (one-way ANOVA followed by Tukey's multiple-comparison test; $P < 0.05$)
@ *vs.* the LPS group (one-way ANOVA followed by Tukey's multiple-comparison test; $P < 0.05$)

Effect of IMA on BALF Inflammatory Biomarkers

Table 5 depicts the effect of IMA on BALF inflammatory biomarkers. Marked elevations in the BALF contents of TNF-α (3.3-fold), IL-1β (3.1-fold), and IFN-γ (4-fold) were observed after administration of LPS as compared to the control group. Conversely, a significant decrease in BALF content of IL-10 was shown after LPS administration by 48.7% as compared to the control animals. IMA caused significant lowering of TNF-α, IL-1β, and IFN-γ contents as compared to the LPS group by 37.2, 50.6, and 52.5%, respectively. Normalization of the BALF content of IL-10 was detected after treatment with IMA as compared to the control group.

Effect of IMA on BALF Neutrophils Count Contents and Lung Wet/Dry Ratios

Intraperitoneal administration of LPS caused significant augmentation in the BALF neutrophil count (4-fold) contents as compared to the control animals. Meanwhile, a significant increment was revealed after LPS administration

Table 3. Effect of IMA on Kidney Downstream Inflammatory Biomarker Contents in Rats Subjected to LPS

Group	Parameter		
	TNF-α (pg/g tissue)	IL-1β (pg/g tissue)	IL-10 (pg/g tissue)
Control (saline)	39.55 ± 2.42	38.51 ± 1.99	125.3 ± 4.80
LPS	99.78 ± 5.75*	125.4 ± 6.07*	66.53 ± 7.71*
LPS + IMA	62.13 ± 1.94@	64.30 ± 13.16@	92.70 ± 11.78*

Values are expressed as the mean ± SEM of six to eight rats per group
LPS lipopolysaccharide, *IMA* imatinib
* *vs.* the control group (one-way ANOVA followed by Tukey's multiple-comparison test; $P < 0.05$)
@ *vs.* the LPS group (one-way ANOVA followed by Tukey's multiple-comparison test; $P < 0.05$)

in the lung wet/dry weight ratios as compared to the control animals by 1.3-fold. IMA administration normalized the BALF neutrophils count content as compared to the control group. IMA reduced lung wet/dry weight ratios by 31.8% as compared to the LPS group (Fig. 7a, b).

Effect of IMA on LPS-Induced Pathological Changes of the Liver and Kidney

The livers and kidneys, harvested 24 h after the LPS injection, were subjected to H&E staining. The control group showed normal histological structure of the central vein and surrounding hepatocytes in the parenchyma (Fig. 8a) and normal histological structure of the kidney glomeruli and tubules at the cortex (Fig. 9a). In contrast, liver tissues from the LPS-treated group showed severe congestion in the central and portal veins with infiltration of few inflammatory cells in the portal area (Fig. 8b). In addition, kidney tissue of rats subjected to LPS showed congestion in cortical blood vessels and glomerular tufts (Fig. 9b). However, administration of IMA resulted in edema with infiltration of few inflammatory cells in the portal area (Fig. 8c). Kidney sections of the IMA-treated group showed normal histological structure (Fig. 9c).

Table 4. Effect of IMA on Lung Downstream Inflammatory Biomarker Contents in Rats Subjected to LPS

Group	Parameter		
	TNF-α (pg/g tissue)	IL-1β (pg/g tissue)	IL-10 (pg/g tissue)
Control (saline)	31.70 ± 1.33	36.15 ± 1.82	141.1 ± 4.44
LPS	122.1 ± 4.96*	134.3 ± 7.60*	68.9 ± 9.26*
LPS + IMA	82.73 ± 9.29*, @	81.07 ± 11.14*, @	110.9 ± 4.17*, @

Values are expressed as the mean ± SEM of six to eight rats per group
LPS lipopolysaccharide, *IMA* imatinib
* *vs.* the control group (one-way ANOVA followed by Tukey's multiple-comparison test; $P < 0.05$)
@ *vs.* the LPS group (one-way ANOVA followed by Tukey's multiple-comparison test; $P < 0.05$)

DISCUSSION

To the best of our knowledge, this is the first study reporting the beneficial potentials of IMA against LPS-induced sepsis in rats. The remarkable increase in liver serum aminotransferase enzyme activities, ALT and AST, as well as serum levels of sCr and BUN observed in the endotoxemic rats indicates the extensive liver injury and acute kidney injury (AKI) in harmony with previous reports [7, 34]. Considerable amelioration of such hepatic and renal damages was attained by treatment with IMA, as verified by the normalization of both liver and kidney enzyme functions. These results lend support to those of [16] in mice subjected to LPS causing acute liver injury and [35] in hypertensive rats with renal damage.

A main finding in this study is that IMA afforded significant reductions of liver, kidney, and lung tissue NF-κB, P38-MAPK, and STAT-3 protein expressions as compared to the LPS-treated group. NF-κB is an important regulator of immune response to infection; incorrect regulation of NF-κB has been linked to inflammatory diseases and septic shock [36]. Interestingly, it has been reported that protein tyrosine kinase plays a role in induction of cytokines and NF-κB in monocytes after LPS administration [37]. Among the mitogen-activated protein kinases (MAPKs) identified, the P38-MAPK pathway plays a primary role in regulating the expression of inflammatory cytokines [38]. It is well established that the stimulators of P38-MAPK can augment the activity of NF-κB [39].

Hampering of the aforementioned inflammatory mediators by IMA could probably result in diminution of the reactive oxygen species (ROS) generation. According to [40], impairment of the anti-oxidant defense is considered to be critically involved in LPS-induced toxic effects. It is worthy to mention that the ROS cohort causes an increase in the cellular ratio of oxidized/reduced thiol which regulates NF-κB activation [41]. Notably, it has been demonstrated that P38-MAPK stimulation by LPS leads to accumulation of ROS, which leads to prolonged MAPK activation and cell death in a viscous cycle [42]. Additionally,

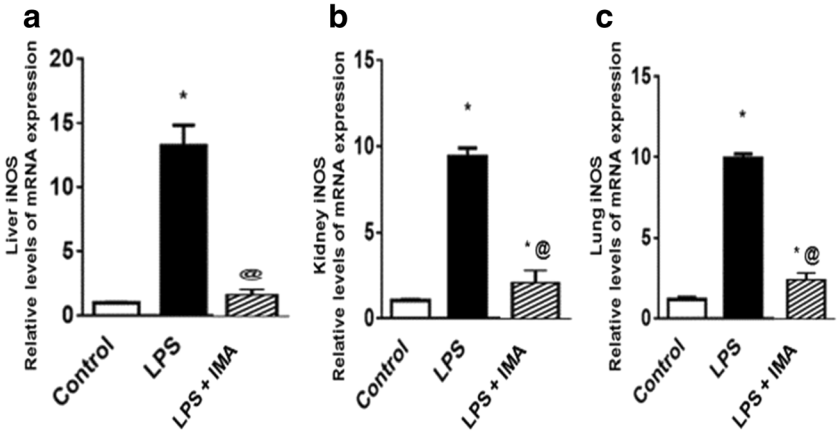

Fig. 5. Effect of IMA on the mRNA expression of liver (**a**), kidney (**b**), and lung (**c**) iNOS contents in rats subjected to LPS. Each bar with a vertical line represents the mean ± SEM of six to eight rats per group. Asterisk, *vs.* the control group and at sign, *vs.* the LPS group (one-way ANOVA followed by Tukey's multiple-comparison test; $P < 0.05$). LPS, lipopolysaccharide; IMA, imatinib; iNOS, inducible nitric oxide synthase.

STAT activation by LPS plausibly occurs indirectly *via* cytokines and/or ROS that are generated by LPS [43].

The present investigation elucidated that treatment with IMA curbed the elevation of TNF-α, IL-1β, and iNOS contents in liver, kidney, and lung tissues; this could be explained in the light of the finding that this tyrosine kinase inhibitor hinders LPS-mediated phosphorylation of the regulatory protein IκB, with subsequent prevention of the transcription factor NF-κB activation [16]. These findings are linked to the fact that IMA suppression of abelson kinase (c-Abl), a non-receptor tyrosine kinase, phosphorylation was accompanied by reduced TNF-α and IL-1β in mice [15]. Besides, IMA significantly diminished BALF TNF-α and IFN-γ levels and this may be attributed to the downregulatory effect of IMA on all T helper 1 (Th1)-specific cytokines [44]. Additionally, LPS-induced IFN-γ production in BALF plays a role in the early edema development and contributes to later lethal events. In a previous study, [45] challenged mice with LPS given intraperitoneally and found that pretreatment with a neutralizing anti-IFN-γ antibody inhibited late (24 h) edema and lethal effects.

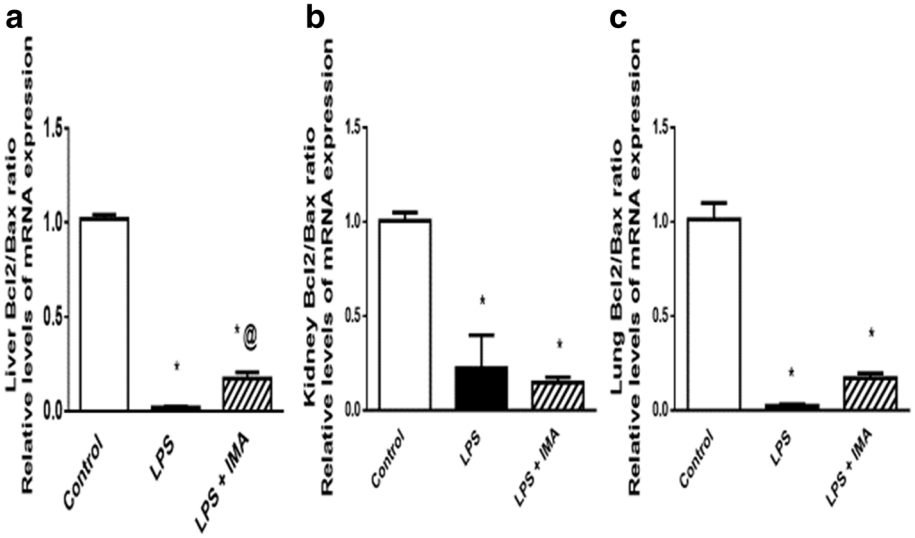

Fig. 6. Effect of IMA on the mRNA expression of liver (**a**), kidney (**b**), and lung (**c**) Bcl2/Bax ratios in rats subjected to LPS. Each bar with a vertical line represents the mean ± SEM of six to eight rats per group. Asterisk, *vs.* the control group and at sign, *vs.* the LPS group (one-way ANOVA followed by Tukey's multiple-comparison test; $P < 0.05$). LPS, lipopolysaccharide; IMA, imatinib; Bcl2, B cell lymphoma 2.

Table 5. Effect of IMA on BALF Biomarkers Contents in Rats Subjected to LPS

Group	Parameter			
	TNF-α (pg/mL)	IL-1β (pg/mL)	IL-10 (pg/mL)	IFN-γ (pg/mL)
Control (saline)	36.03 ± 4.80	40.16 ± 3.89	121.6 ± 6.63	39.99 ± 1.92
LPS	120.5 ± 5.13*	125.5 ± 16.51*	62.38 ± 14.61*	165.4 ± 7.03*
LPS + IMA	75.67 ± 9.85*, @	61.97 ± 2.55*, @	87.60 ± 6.76@	78.63 ± 12.02*, @

Values are expressed as the mean ± SEM of six to eight rats per group
LPS lipopolysaccharide, *IMA* imatinib
* *vs.* the control group (one-way ANOVA followed by Tukey's multiple-comparison test; $P < 0.05$)
@ *vs.* the LPS group (one-way ANOVA followed by Tukey's multiple-comparison test; $P < 0.05$)

The current high lung wet/dry weight ratios, an index of pulmonary edema, observed in the lung tissues of LPS-treated rats indicated substantial lung damage *via* increasing pulmonary vascular permeability [46]. Treatment with IMA ameliorated the pulmonary edema by significant lowering of lung wet/dry weight ratios. Consistent with these results, the IMA-treated mice were prominently protected against LPS-induced lung edema formation [47]. The normalization of the BALF neutrophil content observed in IMA-treated rats indicated an anti-inflammatory role of IMA. Hitherto, the downregulatory effect of IMA on neutrophils has been described by [47].

In this study, the IMA-treated group exhibited normal IL-10 levels in liver, kidney, and lung tissues which could be attributed to an IMA upregulatory effect on T-helper 2 (Th2) cytokines [44]. The anti-inflammatory IL-10 is known to negatively regulate toll-like receptor signaling and is a potent downregulator of cell-mediated immune and pro-inflammatory responses in the LPS murine model of sepsis [48]. IL-10 plays a role in inhibition of the production of pro-inflammatory mediators TNF-α, IL-1β, and nitric oxide (NO) produced by LPS in rats [49]. Furthermore, [50] conveyed that the protective effects against LPS-induced acute lung injury (ALI) in mice are related to reducing the BALF content of TNF-α, while increasing IL-10 secretion and keeping the balance between inflammatory mediators and anti-inflammatory factors. On the contrary, a former study reported the elevation

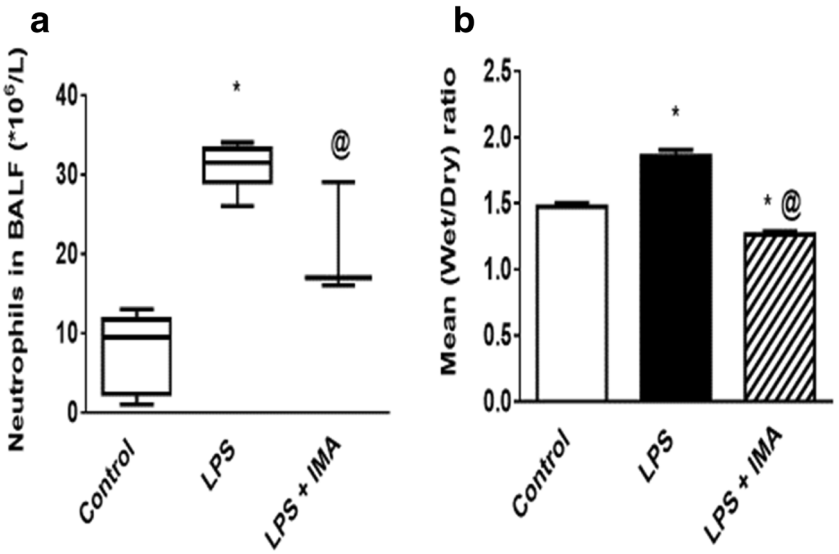

Fig. 7. Effect of IMA on BALF neutrophils count content (**a**) and lung wet/dry weight ratios (**b**) in rats subjected to LPS. Each bar of neutrophils count represents the median of six to eight animals ± (range) (Kruskal-Wallis followed by Dunn's multiple-comparison test). Each bar of lung wet/dry ratios represents the mean of eight animals ± SEM (one-way ANOVA followed by Tukey's multiple-comparison test; $P < 0.05$). Asterisk, *vs.* the control group; at sign, *vs.* the LPS group. LPS, lipopolysaccharide; IMA, imatinib.

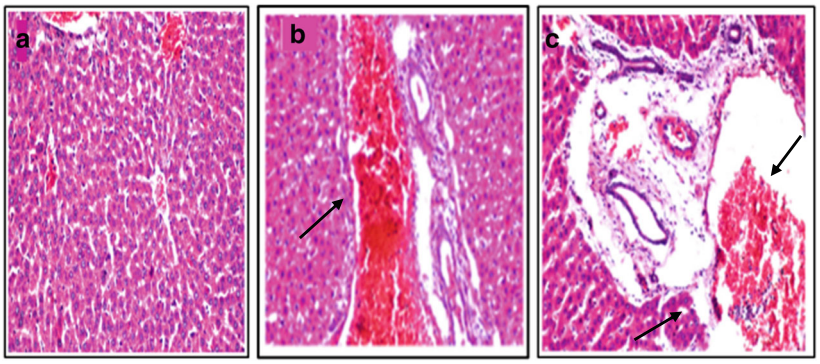

Fig. 8. Photomicrographs of liver sections showing effects of IMA on the liver using hematoxylin and eosin (H&E) stain in rats subjected to LPS (×40): a = Control group, b = LPS-treated group showed severe congestion in the portal and central veins (arrow), and c = LPS + IMA showed edema with few inflammatory cells infiltration in portal area (arrow) with congestion in portal vein (arrow). Where, LPS; lipopolysaccharide, IMA; imatinib.

of BALF IL-10 after LPS administration in rats [51]. Based on that, the precise nature of IL-10 following traumatic injury, shock, and/or sepsis remains controversial. IL-10 also inhibits LPS-induced IFN-γ synthesis as observed *in vivo* in the mice endotoxemia model [52].

The present work supported the idea that apoptosis is a key element in the pathogenesis of sepsis where LPS decreased the anti-apoptotic protein Bcl2 gene expression and increased the apoptotic Bax gene expression in the liver, kidney, and lung, reflecting a significant Bcl2/Bax ratio reduction that promoted cellular apoptosis as compared to control animals. These findings are in line with previous studies of sepsis-induced rat liver [53], kidney [54], and lung [55] injuries. This study showed that IMA significantly increased the Bcl2/Bax ratio in liver and lung tissues; however, it tended to amend the apoptotic protein ratio in the kidney.

In corporation with the biochemical parameters, the histological examination of liver and kidney sections of IMA-treated animals resulted in edema with infiltration of few inflammatory cells in the portal area with congestion in the portal vein, and multiple focal necrosis in hepatic parenchyma. Concerning kidney histopathology, the rats subjected to IMA depicted normal kidney section histological structure in agreement with the findings previously described by [35]. In context, IMA had a potent inhibitory effect on glomerular macrophage (MQ) accumulation and diminished glomerulonephritis induced by the anti-glomerular basement membrane antibody [56]. Contrariwise, LPS-treated rats showed severe congestion in the portal and central veins as well as multiple focal necrosis in the hepatic parenchyma in a diffuse manner and congestion in the cortical blood vessels and glomerular tufts.

In conclusion, this study endorses a curative effect of IMA in the LPS model of sepsis which might be attributed to its anti-inflammatory, anti-oxidant, and anti-apoptotic effects. These beneficial effects open up new horizons to its therapeutic intervention in the SIRS condition.

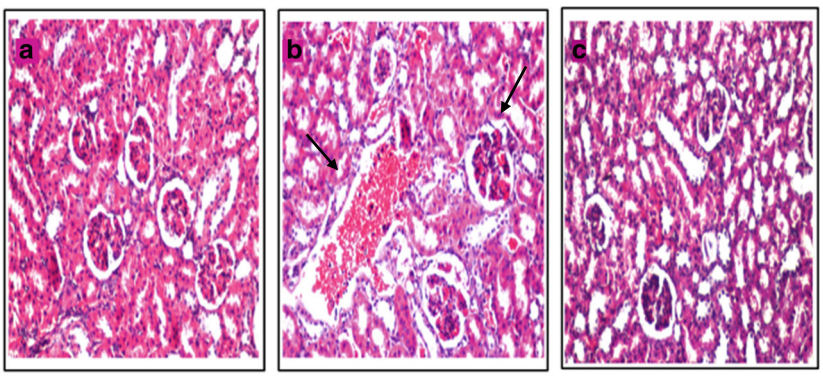

Fig. 9. Photomicrographs of kidney sections showing effects of IMA on the kidney using hematoxylin and eosin (H&E) stain in rats subjected to LPS (×40): **a** control group, **b** LPS-treated group showing congestion in cortical blood vessels and glomerular tufts (arrows), and **c** LPS + IMA showing normal kidney histological structure. LPS, lipopolysaccharide; IMA, imatinib.

ACKNOWLEDGEMENTS

The authors thank Dr. Adel Bakeer Kholoussy, Professor of Pathology, Faculty of Medicine, Cairo University, for examining and interpreting histopathological results. Moreover, the authors are grateful to Dr. Heba Mohammed Diaa, Veterinary Doctor, Animal House, Surgical Department, Faculty of Medicine, Cairo University, for her kind help in isolation of broncho-alveolar lavage fluids.

COMPLIANCE WITH ETHICAL STANDARDS

The investigation was approved by the Ethics Committee for Animal Experimentation of Pharmacy, Cairo University (Permit number: PT 599) and complies with the Guide for Care and Use of Laboratory Animals published by the US National Institutes of Health (NIH Publication No. 85-23, revised 1996).

REFERENCES

1. Russell, J.A. 2006. Management of sepsis. *The New England Journal of Medicine* 355: 1699–1713.
2. Stehr, S.N., and K. Reinhart. 2013. Sepsis as a global health problem—why we need a global sepsis alliance. *Shock* 39: 3–4.
3. Lombardo, E., T. van der Poll, O. DelaRosa, and W. Dalemans. 2015. Mesenchymal stem cells as a therapeutic tool to treat sepsis. *World Journal Stem Cells* 7: 368–379.
4. Su, G.L. 2002. Lipopolysaccharides in liver injury: molecular mechanisms of Kupffer cell activation. *American Journal of Physiology. Gastrointestinal and Liver Physiology* 283: G256–G265.
5. Glaucer, M.P., G. Zanetti, J.D. Baumgartner, and J. Cohen. 1991. Septic shock: pathogenesis. *Lancet* 338: 732–739.
6. Ghosh, S., R.D. Latimer, B.M. Gray, R.J. Harwood, and A. Oduro. 1993. Endotoxin-induced organ injury. *Critical Care Medicine* 21: S19–S24.
7. Takahashi, K., H. Mizukami, K. Kamata, W. Inaba, N. Kato, C. Hibi, and S. Yagihashi. 2012. Amelioration of acute kidney injury in lipopolysaccharide-induced systemic inflammatory response syndrome by an aldose reductase inhibitor, fidarestat. *PloS One* 7: e30134.
8. Ma, L., X.Y. Wu, L.H. Zhang, W.M. Chen, A. Uchiyama, T. Mashimo, and Y. Fujino. 2013. Propofol exerts anti-inflammatory effects in rats with lipopolysaccharide-induced acute lung injury by inhibition of CD14 and TLR4 expression. *Brazilian Journal of Medical and Biological Research* 46: 299–305.
9. Shimazu, R., S. Akashi, H. Ogata, Y. Nagai, K. Fukudome, K. Miyake, and M. Kimoto. 1999. MD-2, a molecule that confers lipopolysaccharide responsiveness on Toll-like receptor 4. *The Journal of Experimental Medicine* 189: 1777–1782.
10. Wiersinga, W.J., S.J. Leopold, D.R. Cranendonk, and T. van der Poll. 2014. Host innate immune responses to sepsis. *Virulence* 5: 36–44.
11. Abreu, M.T., E.T. Arnold, L.S. Thomas, R. Gonsky, Y. Zhou, B. Hu, and M. Arditi. 2002. TLR4 and MD-2 expression is regulated by immune-mediated signals in human intestinal epithelial cells. *The Journal of Biological Chemistry* 277: 20431–20437.
12. Manley, P.W., N. Stiefl, S.W. Cowan-Jacob, S. Kaufman, J. Mestan, M. Wartmann, M. Wiesmann, R. Woodman, and N. Gallagher. 2010. Structural resemblances and comparisons of the relative pharmacological properties of imatinib and nilotinib. *Bioorganic & Medicinal Chemistry* 18: 6977–6986.
13. Rubin, B.P., M.C. Heinrich, and C.L. Corless. 2007. Gastrointestinal stromal tumour. *Lancet* 369: 1731–1741.
14. Day, E., B. Waters, K. Spiegel, T. Alnadaf, P.W. Manley, E. Buchdunger, C. Walker, and G. Jarai. 2008. Inhibition of collagen-induced discoidin domain receptor 1 and 2 activation by imatinib, nilotinib and dasatinib. *European Journal of Pharmacology* 599: 44–53.
15. Huang, P., X.S. Zhao, M. Fields, R.M. Ransohoff, and L. Zhou. 2009. Imatinib attenuates skeletal muscle dystrophy in mdx mice. *The FASEB Journal* 23: 2539–2548.
16. Wolf, A.M., D. Wolf, H. Rumpold, S. Ludwiczek, B. Enrich, G. Gastl, G. Weiss, and H. Tilg. 2005. The kinase inhibitor imatinib mesylate inhibits TNF-{alpha} production in vitro and prevents TNF-dependent acute hepatic inflammation. *Proceedings of the National Academy of Sciences of the United States of America* 102: 13622–13627.
17. Stephens, R.S., L. Johnston, L. Servinsky, B.S. Kim, and M. Damarla. 2015. The tyrosine kinase inhibitor imatinib prevents lung injury and death after intravenous LPS in mice. *Physiological Reports* 3: e12589.
18. Aman, J., J. van Bezu, A. Damanafshan, S. Huveneers, E.C. Eringa, S.M. Vogel, A.B. Groeneveld, A. Vonk Noordegraaf, V.W. van Hinsbergh, and G.P. van Nieuw Amerongen. 2012. Effective treatment of edema and endothelial barrier dysfunction with imatinib. *Circulation* 126: 2728–2738.
19. Letsiou, E., A.N. Rizzo, S. Sammani, P. Naureckas, J.R. Jacobson, J.G. Garcia, and S.M. Dudek. 2015. Differential and opposing effects of imatinib on LPS- and ventilator-induced lung injury. *American Journal of Physiology. Lung Cellular and Molecular Physiology* 308: L259–L269.
20. Wang, S., M.C. Wilkes, E.B. Leof, and R. Hirschberg. 2005. Imatinib mesylate blocks a non-Smad TGF-beta pathway and reduces renal fibrogenesis in vivo. *The FASEB Journal* 19: 1–11.
21. Yagi, H., A. Soto-Gutierrez, N. Navarro-Alvarez, Y. Nahmias, Y. Goldwasser, Y. Kitagawa, A.W. Tilles, R.G. Tompkins, B. Parekkadan, and M.L. Yarmush. 2010. Reactive bone marrow stromal cells attenuate systemic inflammation via sTNFR1. *Molecular Therapy* 18: 1857–1864.
22. Rossi, F., Y. Yozgat, E. de Stanchina, D. Veach, B. Clarkson, K. Manova, F.G. Giancotti, C.R. Antonescu, and P. Besmer. 2010. Imatinib upregulates compensatory integrin signaling in a mouse model of gastrointestinal stromal tumor and is more effective when combined with dasatinib. *Molecular Cancer Research* 8: 1271–1283.
23. Inami, M., K. Inokuchi, H. Yamaguchi, K. Nakayama, A. Watanabe, N. Uchida, S. Tanosaki, and K. Dan. 2006. Oral administration of imatinib to P230 BCR/ABL-expressing transgenic mice changes clones with high BCR/ABL complementary DNA expression into those with low expression. *International Journal of Hematology* 84: 346–353.
24. Freireich, E.J., E.A. Gehan, D.P. Rall, L.H. Schmidt, and H.E. Skipper. 1966. Quantitative comparison of toxicity of anticancer agents in mouse, rat, hamster, dog, monkey, and man. *Cancer Chemotherapy Reports* 50: 219–244.
25. Cocchetto, D.M., and T.D. Bjornsson. 1983. Methods for vascular access and collection of body fluids from the laboratory rat. *Journal of Pharmaceutical Sciences* 72: 465–492.

26. Mei, S.H., S.D. McCarter, Y. Deng, C.H. Parker, W.C. Liles, and D.J. Stewart. 2007. Prevention of LPS-induced acute lung injury in mice by mesenchymal stem cells overexpressing angiopoietin 1. *PLoS Medicine* 4: e269.
27. Lam, C.F., Y.C. Liu, J.K. Hsu, P.A. Yeh, T.Y. Su, C.C. Huang, M.W. Lin, P.C. Wu, P.J. Chang, and Y.C. Tsai. 2008. Autologous transplantation of endothelial progenitor cells attenuates acute lung injury in rabbits. *Anesthesiology* 108: 392–401.
28. Sims, J.E., and D.E. Smith. 2010. *Nature Reviews. Immunology* 10: 89.
29. Vilcek, J., and T.H. Lee. 1991. Tumor necrosis factor. New insights into the molecular mechanisms of its multiple actions. *The Journal of Biological Chemistry* 266: 7313–7316.
30. Eskdale, J., D. Kube, H. Tesch, and G. Gallagher. 1997. Mapping of the human IL10 gene and further characterization of the 5′ flanking sequence. *Immunogenetics* 46: 120–128.
31. Thiel, D.J., M.H. le Du, R.L. Walter, A. D'Arcy, C. Chene, M. Fountoulakis, G. Garotta, F.K. Winkler, and S.E. Ealick. 2000. Observation of an unexpected third receptor molecule in the crystal structure of human interferon-gamma receptor complex. *Structure* 8: 927–936.
32. Livak, K.J., and T.D. Schmittgen. 2001. Analysis of relative gene expression data using real-time quantitative PCR and the 2(−delta delta C(T)) method. *Methods* 25: 402–408.
33. Bancroft J.D., and A. Stevens. Turner DR. 1996. Theory and practice of histological techniques. In: New York, Churchill, Livingstone. Vol.4th Ed.
34. Sener, G., H. Toklu, C. Kapucu, F. Ercan, G. Erkanli, A. Kacmaz, M. Tilki, and B.C. Yegen. 2005. Melatonin protects against oxidative organ injury in a rat model of sepsis. *Surgery Today* 35: 52–59.
35. Graciano, M.L., and K.D. Mitchell. 2012. Imatinib ameliorates renal morphological changes in Cyp1a1-Ren2 transgenic rats with inducible ANG II-dependent malignant hypertension. *American Journal of Physiology. Renal Physiology* 302: F60–F69.
36. An, J., J. Du, N. Wei, T. Guan, A.K. Camara, and Y. Shi. 2012. Differential sensitivity to LPS-induced myocardial dysfunction in the isolated brown Norway and Dahl S rat hearts: roles of mitochondrial function, NF-kappaB activation, and TNF-alpha production. *Shock* 37: 325–332.
37. Geng, Y., B. Zhang, and M. Lotz. 1993. Protein tyrosine kinase activation is required for lipopolysaccharide induction of cytokines in human blood monocytes. *Journal of Immunology* 151: 6692–6700.
38. Liu, S.H., K. Ma, X.R. Xu, and B. Xu. 2010. A single dose of carbon monoxide intraperitoneal administration protects rat intestine from injury induced by lipopolysaccharide. *Cell Stress & Chaperones* 15: 717–727.
39. Craig, R., A. Larkin, A.M. Mingo, D.J. Thuerauf, C. Andrews, P.M. McDonough, and C.C. Glembotski. 2000. p38 MAPK and NF-kappa B collaborate to induce interleukin-6 gene expression and release. Evidence for a cytoprotective autocrine signaling pathway in a cardiac myocyte model system. *The Journal of Biological Chemistry* 275: 23814–23824.
40. Crespo, E., M. Macias, D. Pozo, G. Escames, M. Martin, F. Vives, J.M. Guerrero, and D. Acuna-Castroviejo. 1999. Melatonin inhibits expression of the inducible NO synthase II in liver and lung and prevents endotoxemia in lipopolysaccharide-induced multiple organ dysfunction syndrome in rats. *The FASEB Journal* 13: 1537–1546.
41. Forman, H.J., and M. Torres. 2001. Redox signaling in macrophages. *Molecular Aspects of Medicine* 22: 189–216.
42. Sakon, S., X. Xue, M. Takekawa, T. Sasazuki, T. Okazaki, Y. Kojima, J.H. Piao, H. Yagita, K. Okumura, T. Doi, and H. Nakano. 2003. NF-kappaB inhibits TNF-induced accumulation of ROS that mediate prolonged MAPK activation and necrotic cell death. *The EMBO Journal* 22: 3898–3909.
43. Severgnini, M., S. Takahashi, L.M. Rozo, R.J. Homer, C. Kuhn, J.W. Jhung, G. Perides, M. Steer, P.M. Hassoun, B.L. Fanburg, B.H. Cochran, and A.R. Simon. 2004. Activation of the STAT pathway in acute lung injury. *American Journal of Physiology. Lung Cellular and Molecular Physiology* 286: L1282–L1292.
44. Adzemovic, M.V., M. Zeitelhofer, U. Eriksson, T. Olsson, and I. Nilsson. 2013. Imatinib ameliorates neuroinflammation in a rat model of multiple sclerosis by enhancing blood-brain barrier integrity and by modulating the peripheral immune response. *PloS One* 8: e56586.
45. Faggiona, R., S. Gatt, M.T. Demetri, R. Delgado, B. Echternacher, P. Gnocchi, H. Heremans, and P. Ghezzi. 1994. Role of xanthine oxidase and reactive oxygen intermediates in LPS- and TNF-induced pulmonary edema. *The Journal of Laboratory and Clinical Medicine* 123: 394–399.
46. Chi, G., M. Wei, X. Xie, L.W. Soromou, F. Liu, and S. Zhao. 2013. Suppression of MAPK and NF-kappaB pathways by limonene contributes to attenuation of lipopolysaccharide-induced inflammatory responses in acute lung injury. *Inflammation* 36: 501–511.
47. Rhee, C.K., J.W. Kim, C.K. Park, J.S. Kim, J.Y. Kang, S.J. Kim, S.C. Kim, S.S. Kwon, Y.K. Kim, S.H. Park, and S.Y. Lee. 2011. Effect of imatinib on airway smooth muscle thickening in a murine model of chronic asthma. *International Archives of Allergy and Immunology* 155: 243–251.
48. Petit-Bertron, A.F., C. Fitting, J.M. Cavaillon, and M. Adib-Conquy. 2003. Adherence influences monocyte responsiveness to interleukin-10. *Journal of Leukocyte Biology* 73: 145–154.
49. Ledeboer, A., J.J. Breve, S. Poole, F.J. Tilders, and A.M. Van Dam. 2000. Interleukin-10, interleukin-4, and transforming growth factor-beta differentially regulate lipopolysaccharide-induced production of pro-inflammatory cytokines and nitric oxide in co-cultures of rat astroglial and microglial cells. *Glia* 30: 134–142.
50. Zhang, Z., D.L. Qin, J.Y. Wan, Q.X. Zhou, S.H. Xiao, and K. Wu. 2008. Effects of asiaticoside on the balance of inflammatory factors of mouse's acute lung injury induced by LPS. *Zhong Yao Cai* 31: 547–549.
51. Xu, X.L., Q.M. Xie, Y.H. Shen, J.J. Jiang, Y.Y. Chen, H.Y. Yao, and J.Y. Zhou. 2008. Mannose prevents lipopolysaccharide-induced acute lung injury in rats. *Inflammation Research* 57: 104–110.
52. Marchant, A., C. Bruyns, P. Vandenabeele, M. Ducarme, C. Gerard, A. Delvaux, D. De Groote, D. Abramowicz, T. Velu, and M. Goldman. 1994. Interleukin-10 controls interferon-gamma and tumor necrosis factor production during experimental endotoxemia. *European Journal of Immunology* 24: 1167–1171.
53. Cai, Y., Z. Zou, L. Liu, S. Chen, Y. Chen, Z. Lin, K. Shi, L. Xu, and Y. Chen. 2015. Bone marrow-derived mesenchymal stem cells inhibits hepatocyte apoptosis after acute liver injury. *International Journal of Clinical and Experimental Pathology* 8: 107–116.
54. Cui, W.Y., A.Y. Tian, and T. Bai. 2011. Protective effects of propofol on endotoxemia-induced acute kidney injury in rats. *Clinical and Experimental Pharmacology & Physiology* 38: 747–754.
55. Demiralay, R., N. Gursan, and H. Erdem. 2013. The effects of erdosteine and N-acetylcysteine on apoptotic and antiapoptotic markers in pulmonary epithelial cells in sepsis. *The Eurasian Journal of Medicine* 45: 167–175.
56. Iyoda, M., T. Shibata, M. Kawaguchi, T. Yamaoka, and T. Akizawa. 2009. Preventive and therapeutic effects of imatinib in Wistar-Kyoto rats with anti-glomerular basement membrane glomerulonephritis. *Kidney International* 75: 1060–1070.